Spontaneous bond dissociation cascades induced by Be_n clusters (n =2,4)

Contribution from Eva Vos, Inés Corral, M. Merced Montero-Campillo, Otilia Mó, José Elguero, Ibon Alkorta and Manuel Yáñez.
Dpto. de Química, Facultad de Ciencias, Módulo 13, and Institute of Advanced Chemical Sciences (IadChem). Universidad Autónoma de Madrid, Campus de Excelencia UAM-CSIC, Cantoblanco, E-28049 Madrid, Spain and Instituto de Química Médica (CSIC), Juan de la Cierva, 3, E-28006 Madrid, Spain.
E-mail: ines.corral@uam.es, manuel.yanez@uam.es, ibon@iqm.csic.es

Supporting Information (a total of 20 pages)
Contents

Multiconfigurational character of complexes between Be clusters and the Lewis bases

With the aim of quantifying the multiconfigurational character of the Be_2L and Be_4L complexes, we have analyzed for all the stationary points of each family of systems the weight of the most important configurations in the SS-CASSCF wave functions and evaluated the multireference diagnostic M, developed by the group of Truhlar.[1]

The results for Be_2-L complexes, collected in Table S1-S3, reveal a strong multireference character for these species along the potential energy curves. This is especially noticeable for the first adduct between the Be_2 cluster and the Lewis bases where the M values oscillate between 0.2-0.3. These results are consistent with the analysis of the contributions of the different configurations to the CASSCF wave functions, which reveals that the configuration which contributes most to the wave function in all the systems is the Hartree-Fock one, with a weight of 75-79%, confirming that multireference approaches are necessary to correctly tackle these reactions. This configuration is followed in weight (0.06-1%) by the configuration corresponding to an electron promotion from the Be *2s* to the Be *2p* orbitals. Even more pronounced is the multiconfigurational character of the TS transferring the first H from the bases to the Be_2 moiety, for which the M values increase for all the systems to 0.4, with the concomitant decrease of the Hartree-Fock wave function to 72-74%.

In the same way, the potential energy profiles of FH, H_2O and NH_3 interacting with the tetraberyllium clusters are also characterized by a high multiconfigurational nature, as shown in Tables S4-S6. Here, except for the last most stable NH_3-Be_4 minima the M diagnostic is comprised between 0.1 and 0.2.

Also interesting, there is a reverse evolution of the multiconfigurational character throughout the potential energy curves of the Be_2 and Be_4 clusters. In general trends, while for the smaller cluster the initial adducts resulting from the direct interaction of the Be_2 moiety and the Lewis base present a very pronounced multiconfigurational character that tends to diminish as the H are transferred from the Lewis base to the Be cluster, the opposite situation is observed in the Be_4 clusters.

Table S1: Weight of the Hartree-Fock and the second most contributing configurations to the CASSCF(6,10)/cc-pVTZ wave function and M values for the stationary points along the dissociation cascade of Be_2-NH_3. (CASSCF(10,14)/cc-pVTZ values within parenthesis).

Structure	M value	Hartree Fock and second configuration weight
a1	0.317 (0.316)	0.770/0.122 (0.752/0.119)
TS_a1_a2	0.403 (0.395)	0.736/0.170 (0.722/0.161)
a2	0.170 (0.181)	0.879/0.065 (0.851/0.070)
TS_a2_a3	0.177 (0.182)	0.875/0.070 (0.856/0.075)
a3	0.030 (0.034)	0.955/0.008(0.932/0.005)

Table S2: Weight of the Hartree-Fock and the second most contributing configurations to the CASSCF(8,12)/cc-pVTZ wave function and M values for the stationary points along the dissociation cascade of Be_2-H_2O.

Structure	M value	Hartree Fock and second configuration weight
w1	0.324	0.760/0.127
TS_w1_w2	0.404	0.729/0.170
w2	0.190	0.861/0.078
TS_w2_w3	0.167	0.863/0.058
w3	0.032	0.956/0.005

Table S3: Weight of the Hartree-Fock and the second most contributing configurations to the CASSCF(6,10)/cc-pVTZ wave function and M values for the stationary points along the dissociation cascade of Be_2-FH.

Structure	M value	Hartree Fock and second configuration weight
fh1	0.211	0.794/0.057
TS_fh1_fh2	0.402	0.737/0.172
fh2	0.191	0.876/0.081

Table S4: Weight of the Hartree-Fock and the second most contributing configurations to the CASSCF(6,9)/cc-pVTZ wave function and M values for the stationary points along the dissociation cascade of Be_4-NH_3. (CASSCF(12,15)/cc-pVTZ values within parenthesis).

Structure	M value	Hartree Fock and second configuration weight
A1	0.117 (0.123)	0.810/0.008 (0.787/0.008)
TS_A1_A2	0.141 (0.157)	0.804/0.035 (0.760/0.035)
A2	0.118 (0.117)	0.863/0.030 (0.834/0.024)
TS_A2_A3	0.145 (0.147)	0.847/0.046 (0.813/0.043)
A3	0.136 (0.144)	0.876/0.052 (0.841/0.051)
TS_A3_A4	0.187 (0.206)	0.875/0.082 (0.803/0.089)
A4	0.131 (0.133)	0.853/0.020 (0.821/0.020)
TS_A4_A5	0.150 (0.161)	0.845/0.032 (0.815/0.037)
A5	0.238 (0.231)	0.853/0.115 (0.826/0.106)

Table S5: Weight of the Hartree-Fock and the second most contributing configurations to the CASSCF(10,13)/ cc-pVTZ wave function and M values for the stationary points along the dissociation cascade of Be_4-H_2O.

Structure	M value	Hartree Fock and second configuration weight
W1	0.123	0.795/0.009
TS_W1_W2	0.142	0.784/0.031
W2	0.122	0.840/0.036
TS_W2_W3	0.128	0.832/0.027
W3	0.174	0.842/0.070
TS_W3_W4	0.126	0.873/0.047
W4	0.150	0.832/0.022

Table S6: Weight of the Hartree-Fock and the second most contributing configurations to the CASSCF(8,11)/cc-pVTZ wave function and M values for the stationary points along the dissociation cascade of Be_4-FH.

Structure	M value	Hartree Fock and second configuration weight
FH1	0.120	0.804/0.008
TS_FH1_FH2	0.137	0.797/0.032
FH2	0.114	0.850/0.027
TS_FH2_FH3	0.141	0.826/0.0185
FH3	0.119	0.804/0.008

The multiconfigurational nature is not exclusive of the Be_2 and Be_4 complexes. The isolated Be_2 and Be_4 clusters present also an important multireference nature, see Table S7. Obviously, this is not the case of the ligands FH, H_2O and NH_3 whose wave functions are clearly monoreferential, with Hartree-Fock weights ca. 97% (see Table S7).

Table S7: Weight of the Hartree-Fock and the second most contributing configurations to the CASSCF/cc-pVTZ wave function and M values for Be_2, Be_4, FH, H_2O and NH_3. The size of the active spaces are indicated within parenthesis.

Structure	M value	Hartree Fock configuration weight
Be_4 (6,9)	0.125	0.797
Be_2 (4,8)	0.199	0.804
NH_3 (8,7)	0.022	0.967
H_2O (8,6)	0.023	0.977
HF (8,5)	0.021	0.989

The above wave function analysis brings forward that the use of multireference methods is crucial to correctly describe the interaction of Be_2 and Be_4 with Lewis bases.

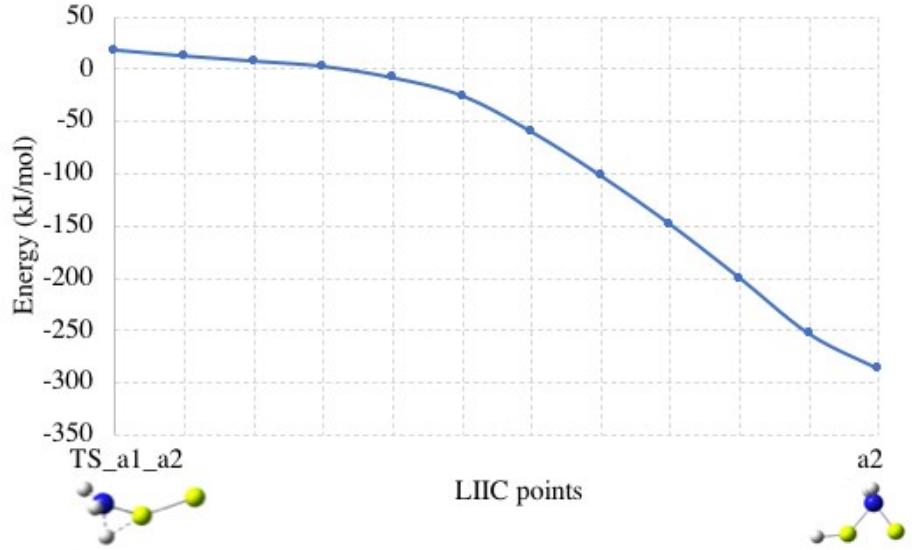

Figure S1. Energetic evolution from TS_a1_a2 towards the local minimum a2 obtained using a linear interpolation procedure at CASPT2(6,10)/cc-pVTZ level.

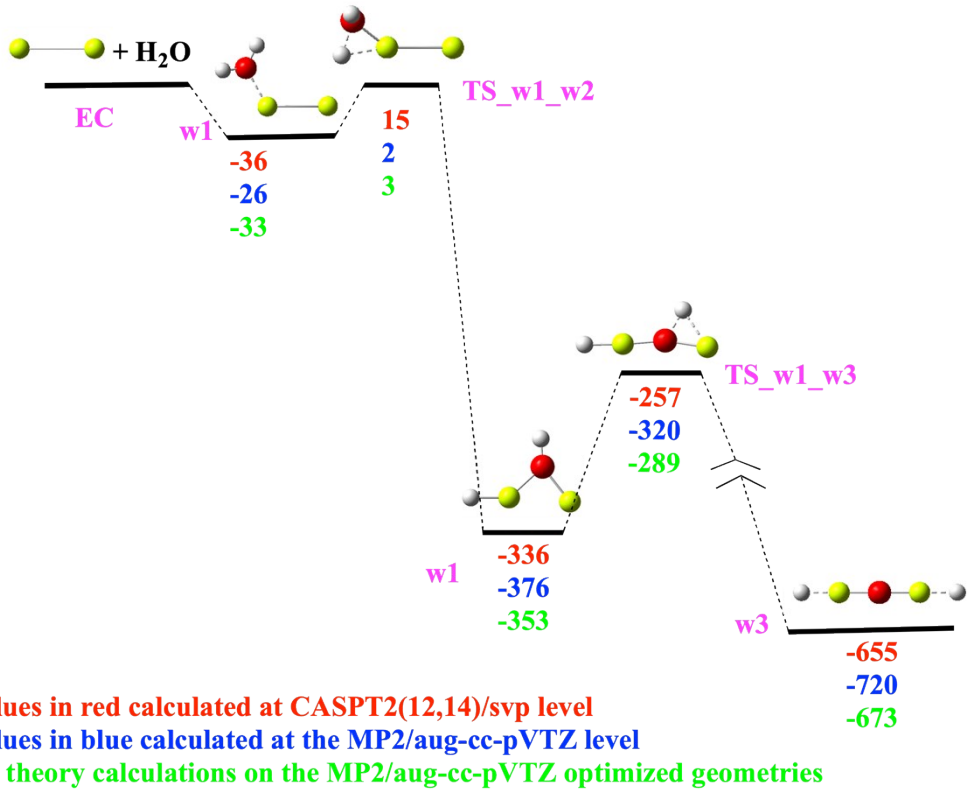

Figure S2. Schematic gas-phase potential energy profile for the interaction between Be_2 and water obtained using different formalisms. Energies relative to the entrance channel (**EC**) are in $kJ \cdot mol^{-1}$.

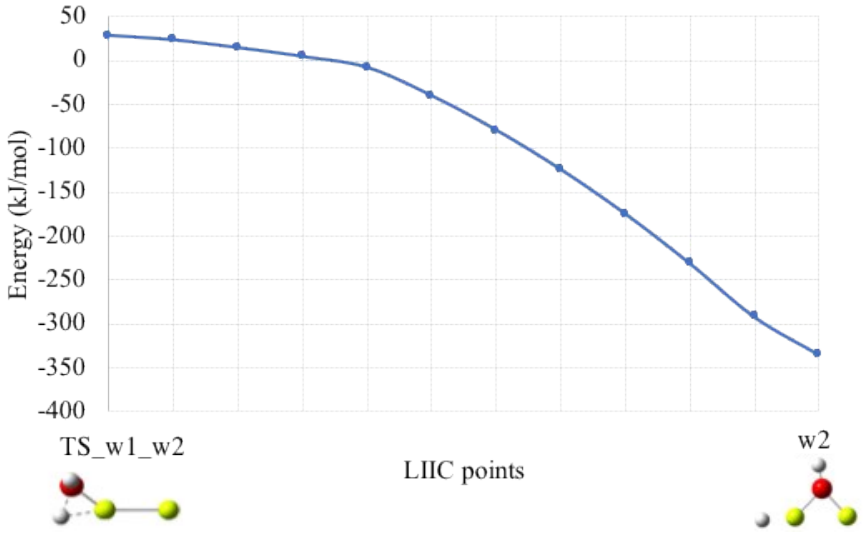

Figure S3. Energetic evolution from TS_w1_w2 towards the local minimum w2 obtained using a linear interpolation procedure at CASPT2(6,10)/cc-pVTZ level.

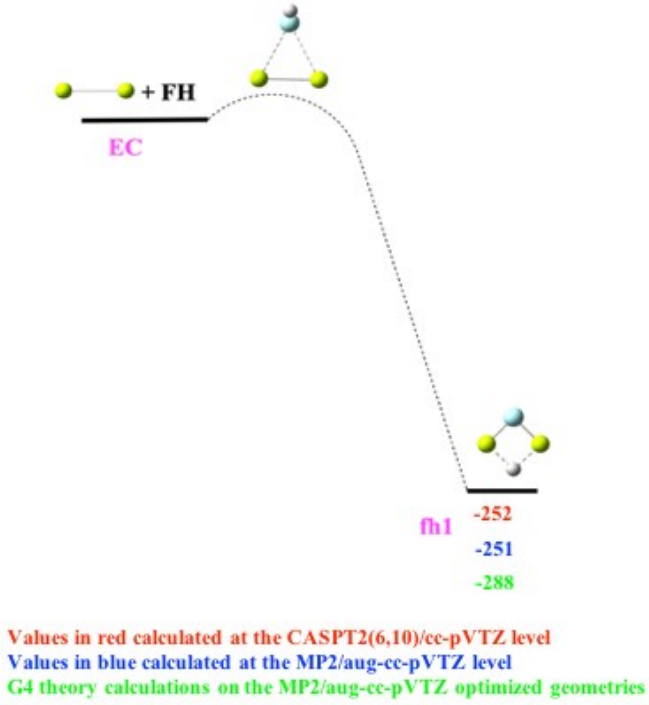

Figure S4. Schematic gas-phase potential energy surface for the interaction between Be_2 and hydrogen fluoride obtained using different formalisms. Energies relative to the entrance channel (**EC**) are in $kJ \cdot mol^{-1}$. In this case, the interaction between the two reactants leads directly to the minimum **fh1** in a practically barrierless process (barrier below 6 $kJ \cdot mol^{-1}$)

Figure S5. Energetic evolution from TS_fh1_fh2 towards the local minimum fh2 obtained using a linear interpolation procedure at CASPT2(6,10)/cc-pVTZ level.

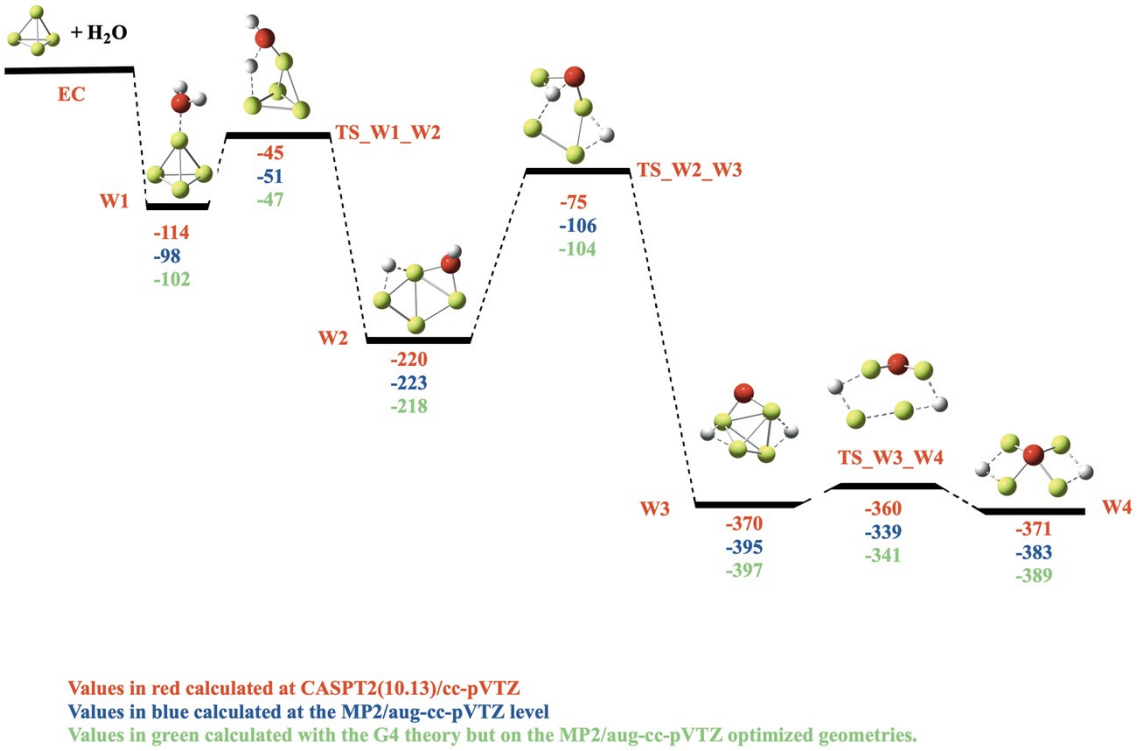

Figure S6. Schematic gas-phase potential energy profile for the interaction between Be_4 and water obtained using different formalisms. Energies relative to the entrance channel (**EC**) are in $kJ \cdot mol^{-1}$.

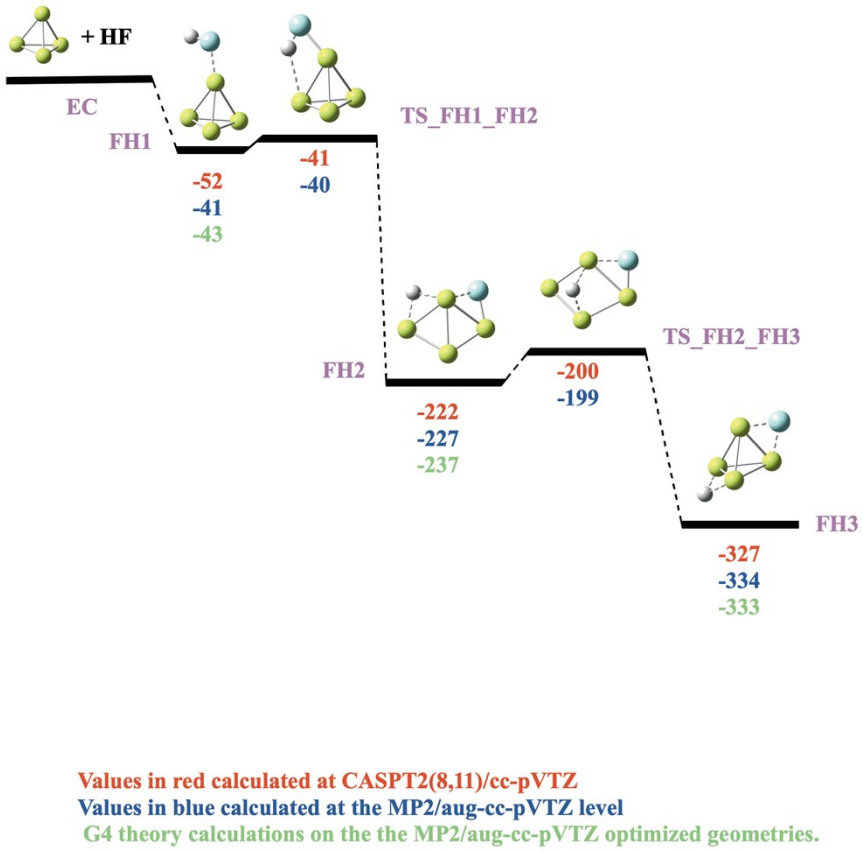

Figure S7. Schematic gas-phase potential energy profile for the interaction between Be_4 and hydrogen fluoride obtained using different formalisms. Energies relative to the entrance channel (**EC**) are in $kJ \cdot mol^{-1}$.

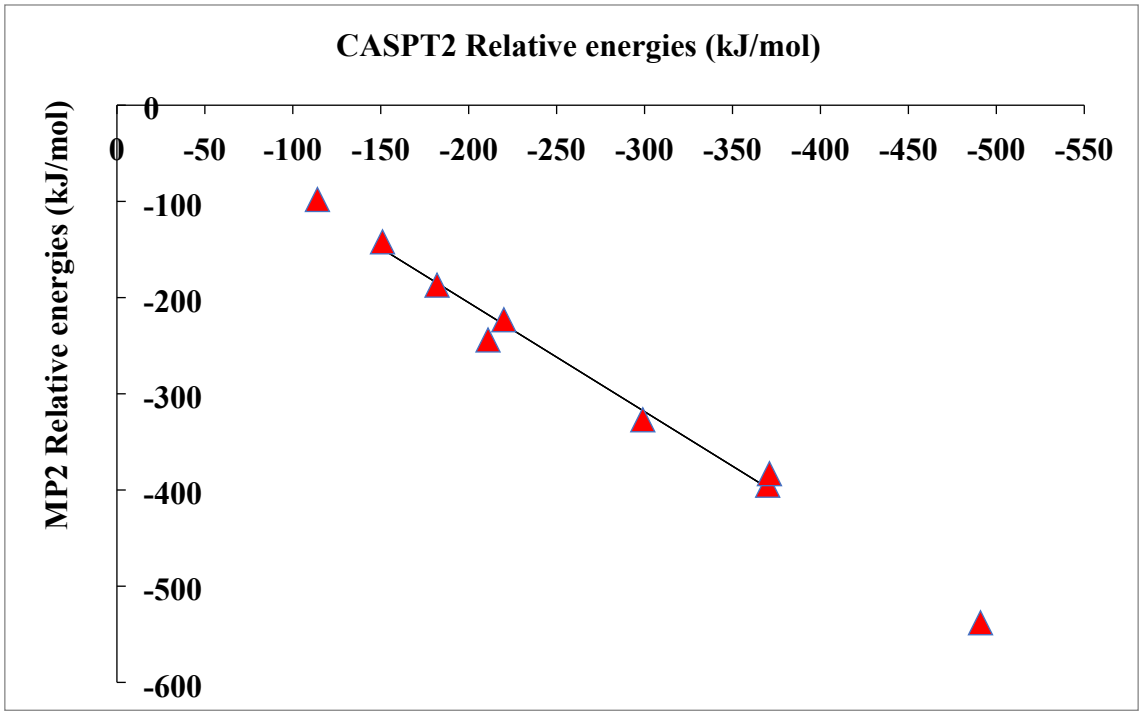

Figure S8. Correlation between MP2/aug-cc-pVTZ and CASPT2/cc-pVTZ relative energies (RE) for clusters of ammonia and water with Be_4. The linear correlation obeys the equation:
RE(MP2) = 1.133 RE(CASPT2) + 21.39 R^2 =0.992

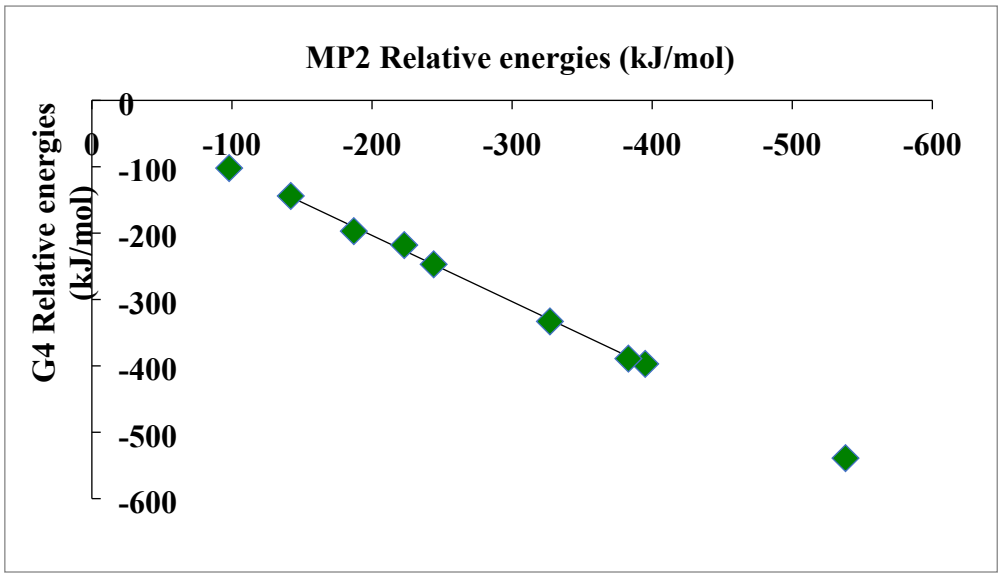

Figure S9. Correlation between G4 and MP2/aug-cc-pVTZ relative energies (RE) for clusters of ammonia and water with Be_4. The linear correlation obeys the equation:
RE(G4) = 0.997 RE(MP2) - 3.98 R^2 =0.999

Computational Details

The CASSCF orbitals included in the active spaces (electrons, orbitals) employed for the Be_2-NH_3, Be_2-H_2O and Be_2-FH calculations, are shown in Figs. S10-S13, respectively.

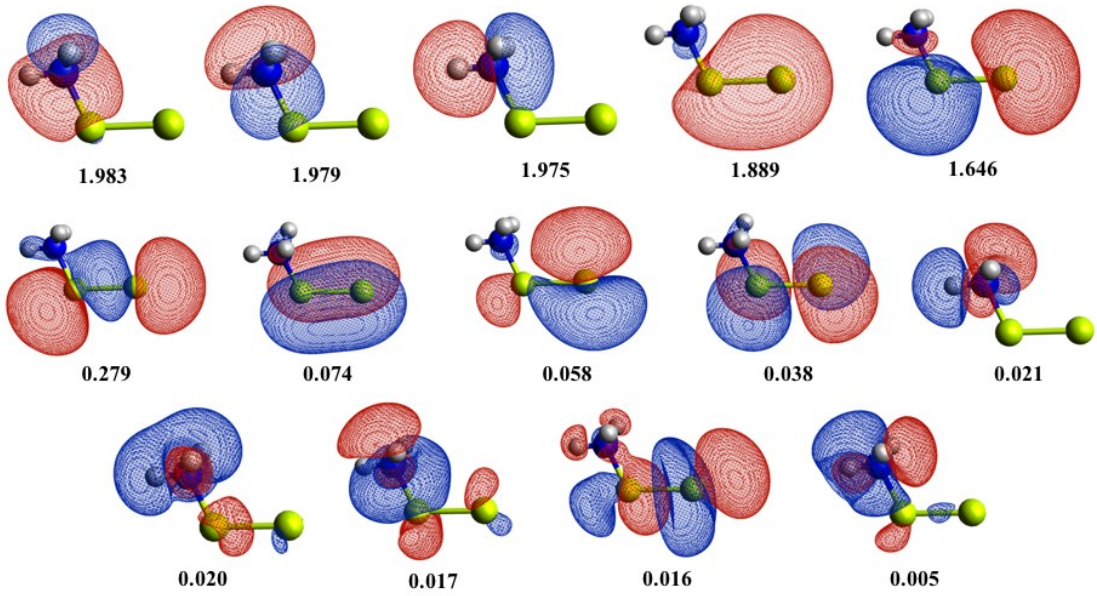

Figure S10. CASSCF orbitals with their occupation numbers included in the (10,14) active space for Be_2-NH_3 at the a1 structure, used in the single point calculation.

Due to the unaffordable cost of the Be_2-NH_3 gradients with the (10,14) active space (Figure S10), the optimization of the stationary points for this system was performed with the reduced (6,10) active space (Figure S11), which conserves the Be_2 , σBe-N and σ*Be-N orbitals.

However, final energies for this cluster were evaluated with the larger active space (10,14).

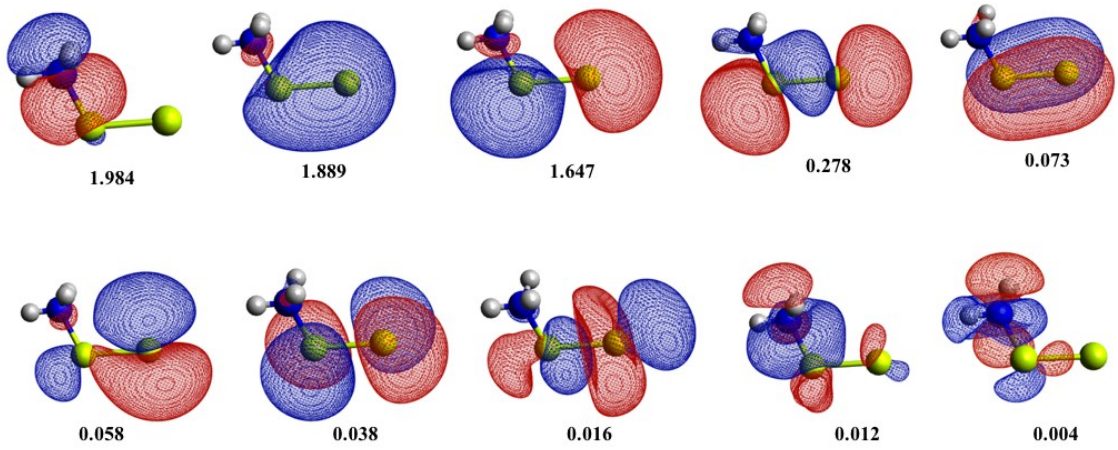

Figure S11. CASSCF orbitals with their occupation numbers included in the (6,10) active space of Be_2-NH_3 at the a1 structure, used in the geometry optimizations.

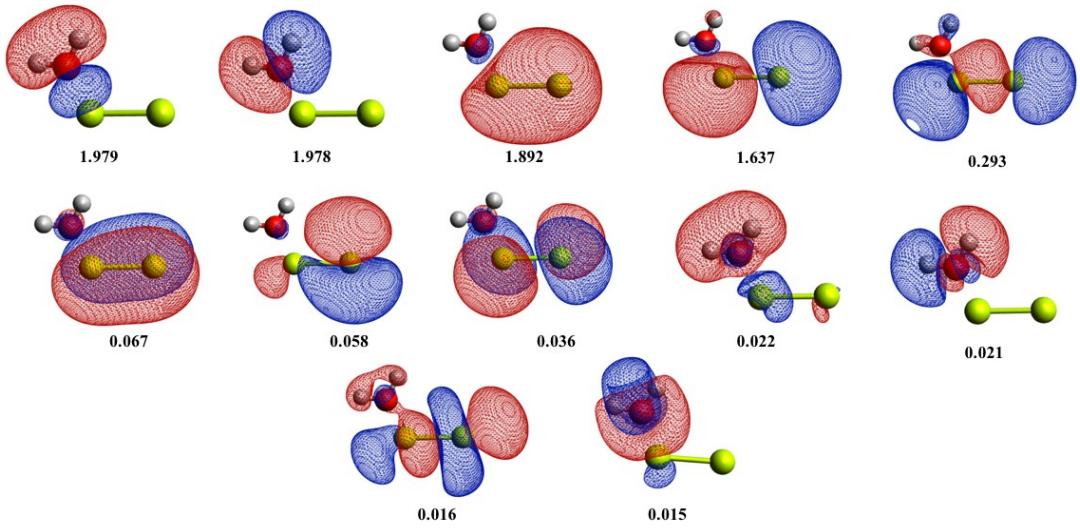

Figure S12. CASSCF orbitals with their occupation numbers included in the (8,12) active space of Be_2-H_2O at the w1 structure.

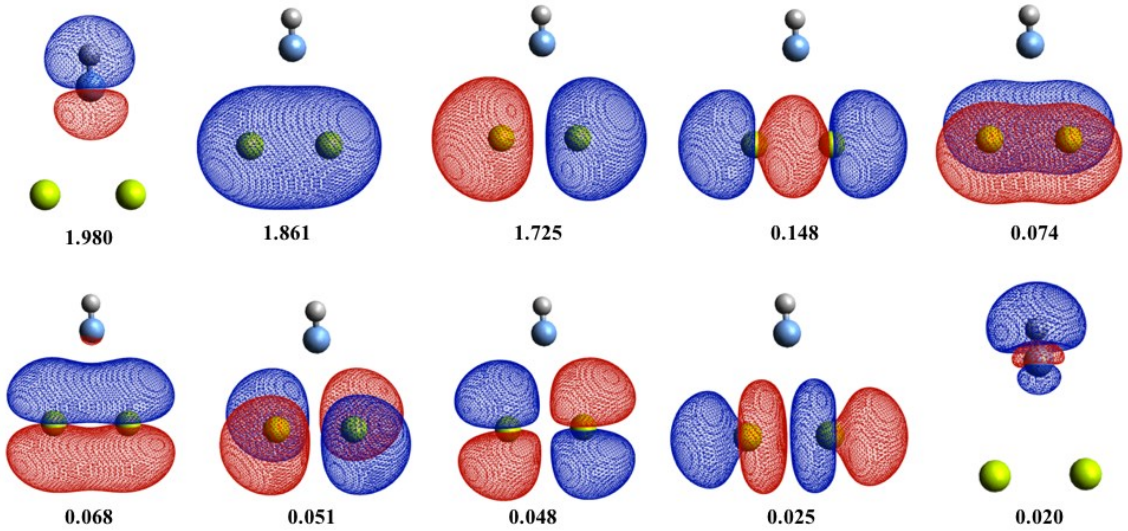

Figure S13. CASSCF orbitals with their occupation numbers included in the (6,10) active space of Be_2-FH at the fh1 structure.

The CASSCF orbitals included in the active spaces used for the Be_4-NH_3, Be_4-H_2O and Be_4-FH, systems, are shown in Figs. S14-S17, respectively.

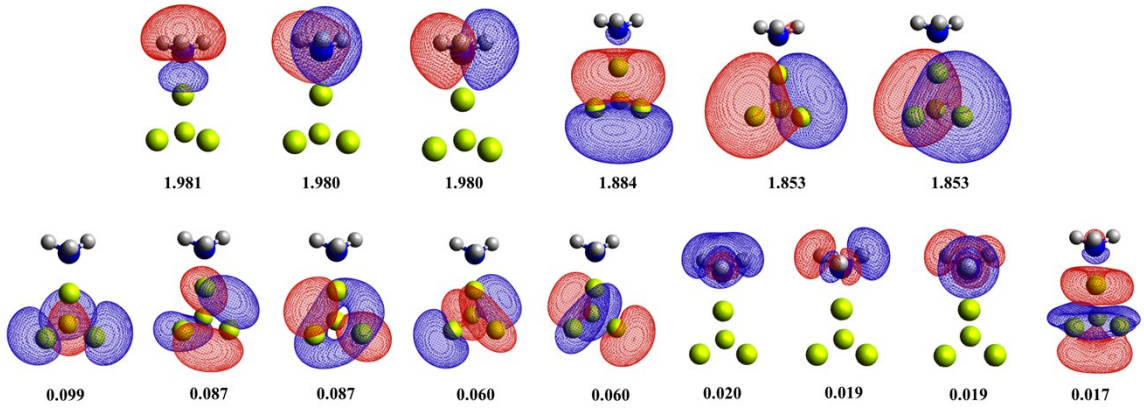

Figure S14. CASSCF orbitals with their occupation numbers included in the (12,15) active space of Be_4-NH_3 at the A1 structure.

Due to the unaffordable cost of the Be_4-NH_3 gradients with the (12,15) active space (Figure S14), the optimization of the stationary points for this system was performed with the reduced (6,9) active space (Figure S15), which only conserves the Be_4 orbitals. However, final energies for this cluster were evaluated with the larger active space (12,15).

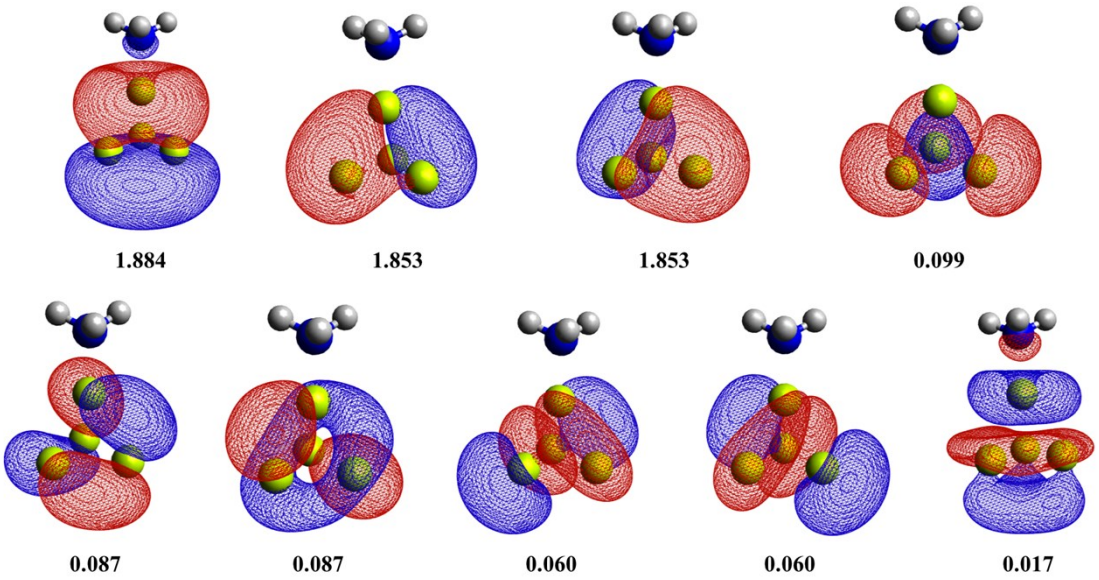

Figure S15. CASSCF orbitals with their occupation numbers included in the reduced (6,9) active space of Be_4-NH_3 at the A1 structure.

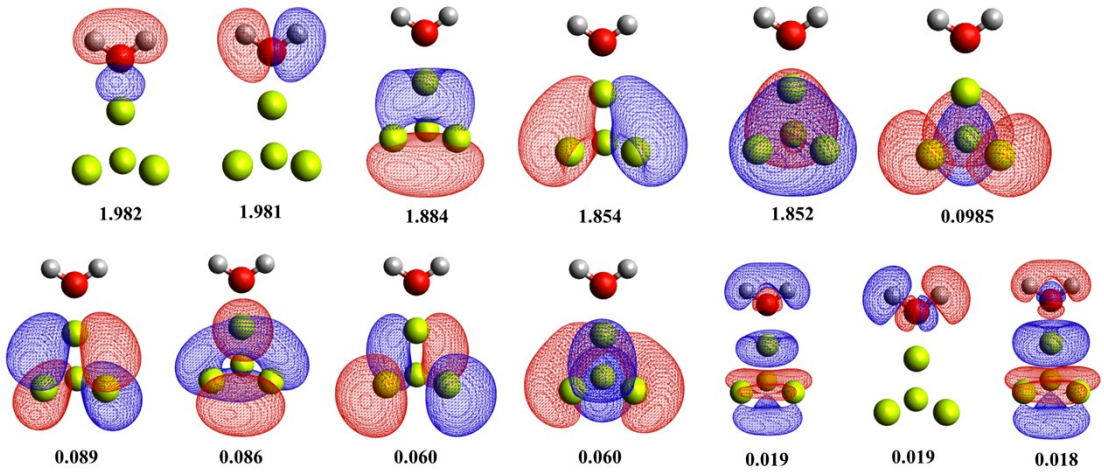

Figure S16. CASSCF orbitals with their occupation numbers included in the (10,13) active space of Be_4-H_2O at the W1 structure.

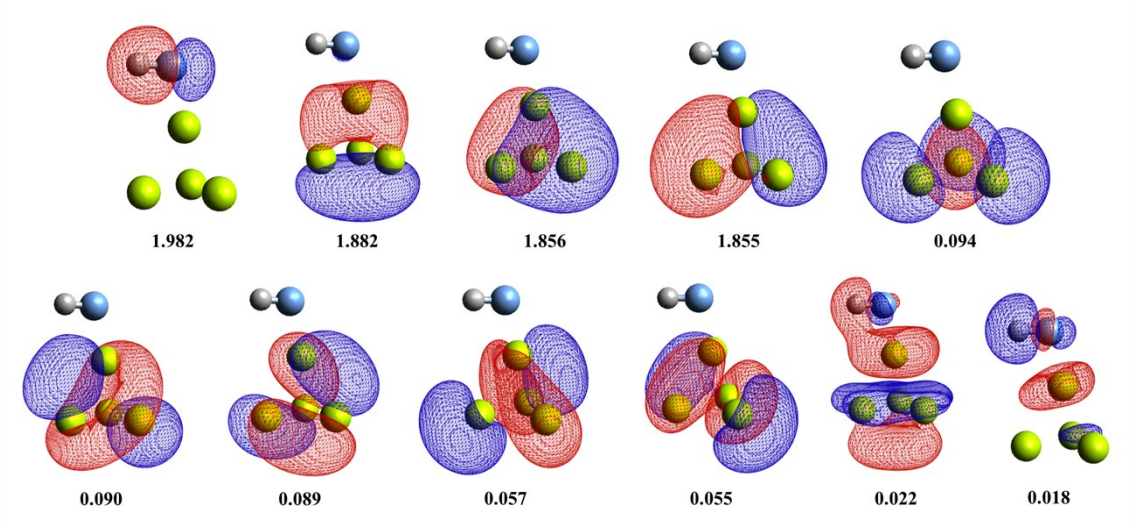

Figure S17. CASSCF orbitals with their occupation numbers included in the (8,11) active space of Be_4-FH at the FH1 structure.

With the aim of preserving the active space throughout the cascade of reactions, linear interpolation in internal coordinates (LIIC) calculations at SS-CASPT2 level were computed between the stationary points optimized at the MP2 level of theory, which were later fully reoptimized at the SS-CASPT2 level.

Besides the Be_2-L and Be_4-L complexes, the isolated molecules, Be_2, Be_4, NH_3, H_2O and FH were also optimized at SS-CASPT2 level and their wave functions were taken as a reference for the bonding analysis. Thus, for Be_2 the (4,8) active space, in Figure S18, is comparable to the active spaces employed in the CASSCF calculations for the Be_2-L complexes, after removing the σ and σ* orbitals of the ligands. The (6,9) active space used for the Be_4 cluster is equivalent to the active spaces employed in the CASSCF calculations for the Be_4-L complexes, after removing the σ and σ* orbitals of the ligands. (Figure S19). For isolated ligands, FH, H_2O and NH_3, an active space including all the lone pair of the heteroatoms and the linear combinations between the *1s* orbitals of the hydrogen atoms and the *2p* orbitals of the F, O or N atoms, leading to the σ and σ* orbitals, was employed.

All the multireference calculations were performed with the 1.2.2 version of Bagel[2] program.

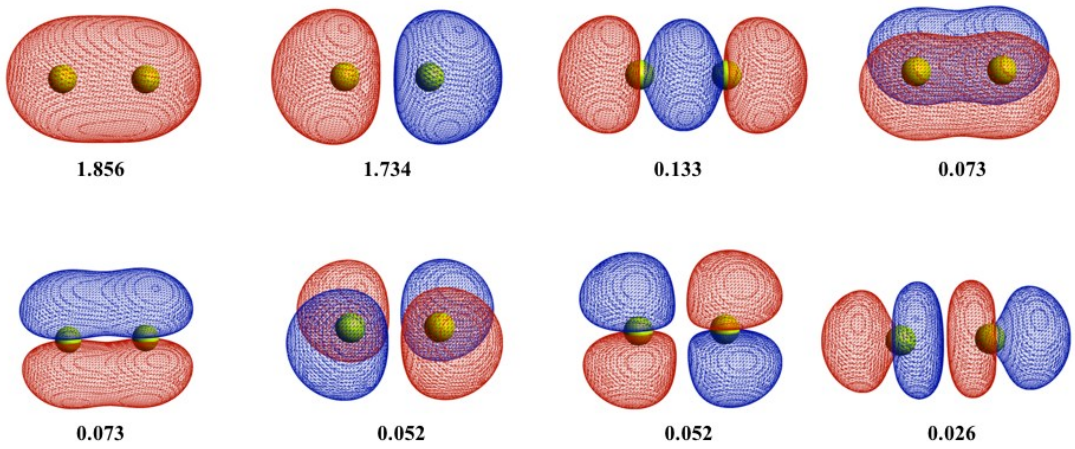

Figure S18. CASSCF orbitals with their occupation numbers included in the (4,8) active space of the isolated Be_2 cluster.

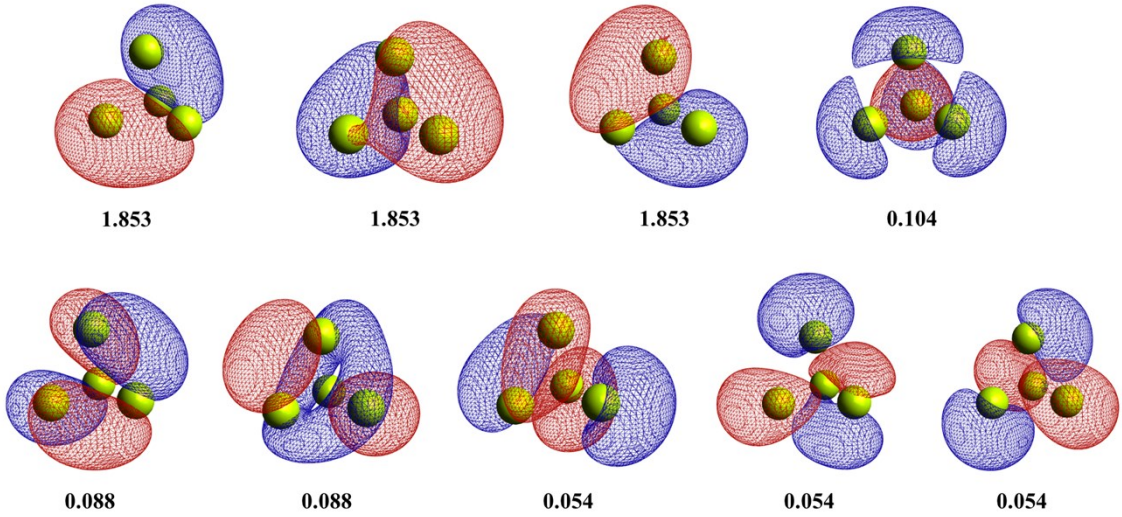

Figure S19. CASSCF orbitals with their occupation numbers included in the (6,9) active space of the isolated Be_4 cluster.

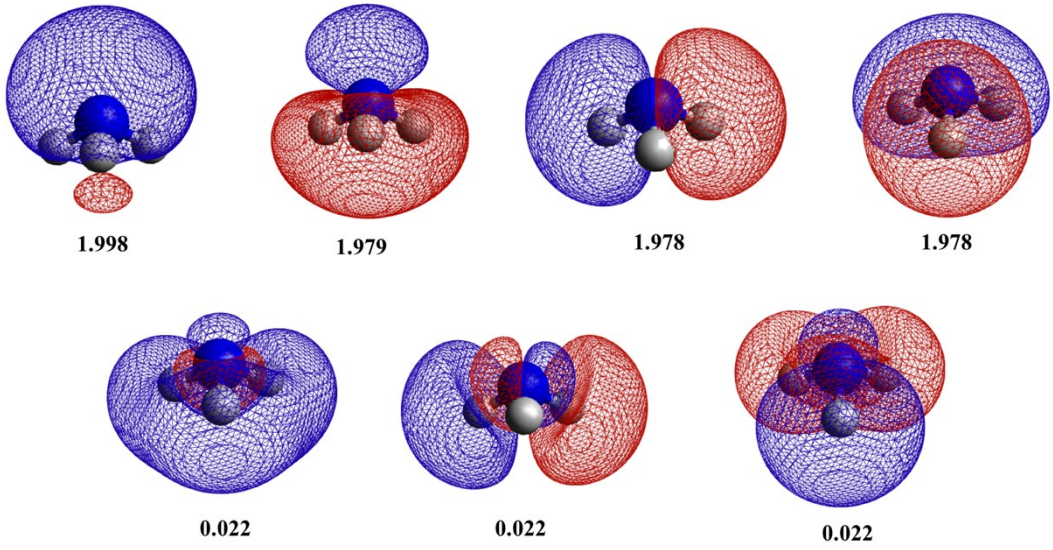

Figure S20. CASSCF orbitals with their occupation numbers included in the (8,7) active space of the isolated NH_3 molecule.

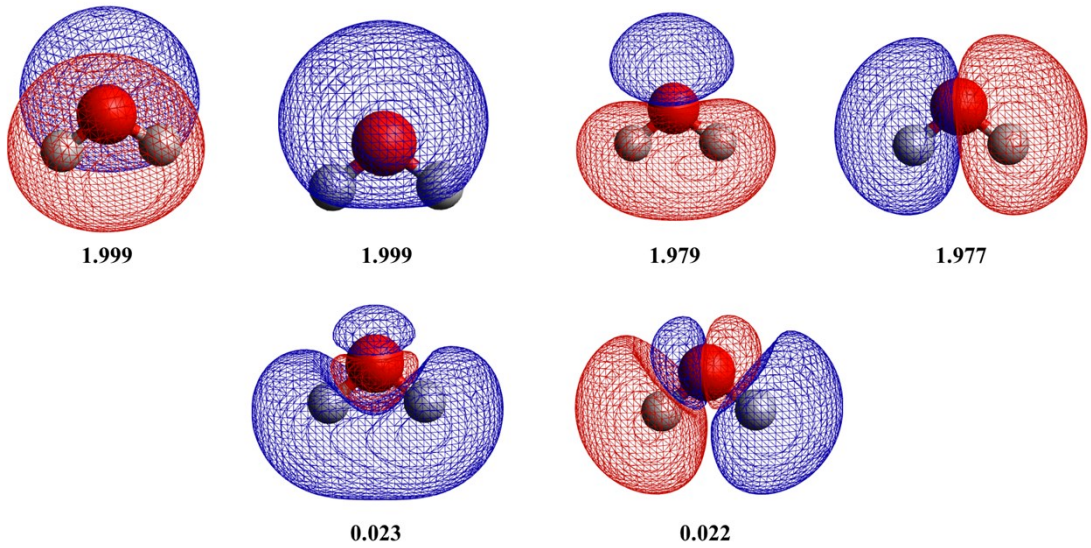

Figure S21. CASSCF orbitals with their occupation numbers included in the (8,6) active space of the isolated H_2O molecule.

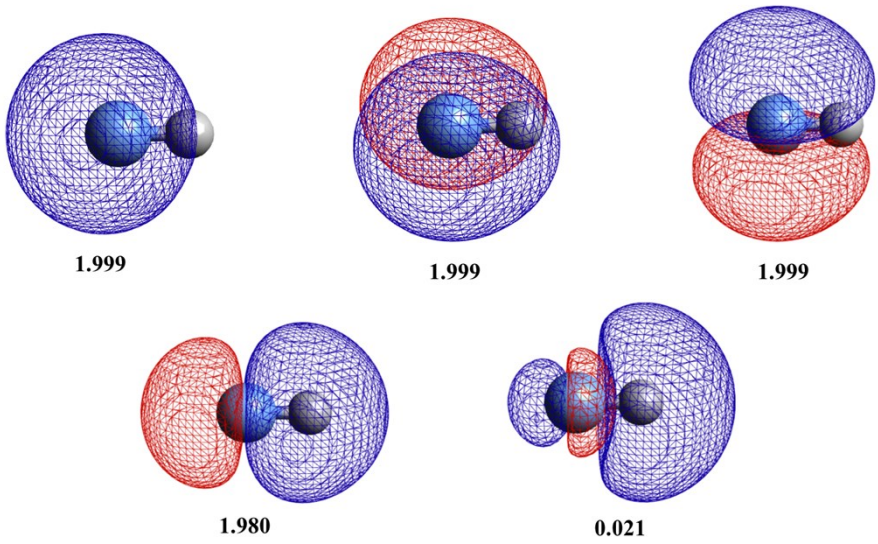

Figure S22. CASSCF orbitals with their occupation numbers included in the (8,5) active space of the isolated FH molecule.

Topological tools. The Non-Covalent Interaction (NCI) index is a method based on the use of the reduced density gradient that allows to find regions in the real space where these interactions do actually take place. This method is implemented in the NCIPLOT program.[3] The abovementioned regions present low *s* (reduced density gradient) and ρ (density) values that can be visualized through 2D and 3D representations. In a 2D diagram representing *s* versus (sign λ_2)·ρ, where λ_2 is the second eigenvalue of the Hessian, interactions appear as steep peaks at negative (sign λ_2)·ρ values (attractive interactions) or positive (sign λ_2)·ρ values (repulsive interactions). Regarding 3D representations, colored isosurfaces are used where (sign λ_2)·ρ values are plotted on *s* isosurfaces. This allows to easily visualize in the real space strongly attractive interactions (blue), strongly repulsive interactions (red) and weakly attractive or repulsive interactions (green) within the van der Waals range. By default, *s* values of 0.3 are represented. In this communication, we have used the latest version of the code, NCIPLOT 4.0, provided by the developers.[4]

A very well known density-based method is QTAIM, the Quantum Theory of Atoms in Molecules[5], implemented in the AIMall program.[6] This method allows to determine the existence and nature of bonding interactions, as interacting atoms give place to a bond critical point (BCP) characterized by a given electron density, which corresponds from a topological point of view with a (3,-1) saddle point. We have also used the electron

localization function (ELF),[7] a topological tool that provides a Lewis picture of a chemical system, dividing the space in basins of different kinds associated to the atomic cores, bonding regions or lone pair regions in which the electron population can be estimated. Polysynaptic basins are shared by two or more atoms, whereas monosynaptic basins belong to only one atom. A color code is used to distinguish between basins: green (bonding polysynaptic basins), yellow (basins including hydrogen) and red (lone pairs). Due to the RHF-UHF instability found for Be_4 and its complexes, the atoms in molecules (AIM), the electron localization function (ELF) [7] and the non-covalent interaction (NCI) analyses were done using the CASSCF wave function obtained in our multireference calculations.

References

1 O. Tishchenko, J. Zheng, D. G. Truhlar, *J. Chem. Theory Comput.,* 2008, **4**, 1208.

2 T. Shiozaki, *WIREs Comput. Mol. Sci.,* 2018, **8,** e1331.

3 a) J. Contreras-García, E. R. Johnson, S. Keinan, R. Chaudret, J. P. Piquemal, D. N. Beratan, W. T. Yang, *J. Chem. Theory Comput,* 2011, **7**, 625; b) E. R. Johnson, S. Keinan, P. Mori-Sanchez, J. Contreras-Garcia, A. J. Cohen, W. T. Yang, *J. Am. Chem. Soc.,* 2010, **132**, 6498.

4 Roberto A. Boto, Francesca Peccati, Rubén Laplaza, Chaoyu Quan, Alessandra Carbone, Jean-Philip Piquemal, Yvon Maday, J. Contreras-García, *J. Chem. Theory Comput.* 2020, **16**, 4150.

5 R. F. W. Bader, *Chem. Rev.,* 1991, **91**, 893.

6 T. A. Keith, AIMAll (Version 13.05.06) Gristmill Software, Overland Park, KS, 2013; aim.tkgristmill.com., 2013.

7 A. Savin, R. Nesper, S. Wengert, T. F. Fassler, *Angew. Chem. Int. Ed.,* 1997, **36**, 1809.